ME547 Midterm Report: Modeling and Simulating a Vectored Thrust Aircraft

Tyler Freitas
ME547 student
University of Washington
Seattle, WA, USA
tfreita@uw.edu

***Abstract*—The following analysis models a 2D vectored thrust aircraft and simulates its positional response with different thruster inputs. This nonlinear model is derived from Newtons' laws of motion and linearized around its equilibrium points using Jacobian Linearization and small angle approximation. This simulation determined the aircraft's positional responses by testing a step, an impulse, and a sine wave at different frequencies. The simulation showed the aircraft's horizontal position is unstable for all inputs. The large change in the aircraft orientation violated the small angle approximation, and the model neglected air torque resistance. The vertical position was stable for an impulse input but not asymptotically stable for a step and sinusoidal inputs. The next step for this analysis will be implementing a Linear-Quadratic Regulator (LQR) controller to maintain stability.**

I. Introduction

The study of motion controls can be explored in many mechanical system applications. Motion controls have been implemented on aircraft for many years to control structural components including ailerons, elevators, and rudders. In recent decades, the Harrier jump jet has introduced the possibility of vertical takeoff and landing [1]. Specifically, the direction of the thrusters changes from a horizontal to a downward position [1]. To navigate these vertical maneuvers, a controller is implemented for positional stability [3],[1]. This paper will focus on creating a model and simulating the response of a hovering vectored thrust aircraft.

II. Problem Formation:

A. Model/Plant

The model (plant) of this system is a vectored thrust aircraft, which is analyzed as a rigid body in 2D space. This model has 3 thrusters: 1 thruster passing through the aircraft centroid, and 2 angled thrusters near the wingtips [1]. Note that these wingtip thrusters are used for aircraft stability [1]. These 3 thrusters are coupled together and move as a unit. Therefore, the changes in the wingtip thruster angles are the same. Fig. 1 displays the free body diagram (FBD) of the plant. This diagram is in the Cartesian Coordinates System. The system outputs are the aircraft position (x, y) and orientation (θ). Note that the simulation outputs are only the horizontal (x) and vertical (y) positions. The reaction forces of the thrusters are translated to a common intersection point, and r is the distance from this common intersection point of the thrusters to the aircraft centroid [1]. Additionally, these reaction forces are combined and broken down into horizontal (F_1) & vertical (F_2) components which are the inputs for this plant. The other arrows in this FBD are the applied thruster forces. Note that this FBD neglects air drag forces.

B. Free-Body Diagram

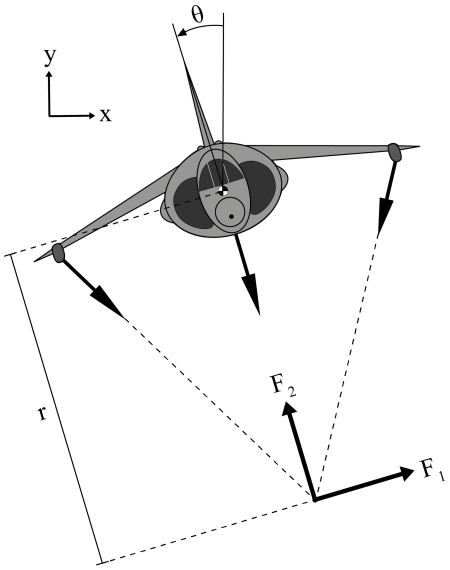

Fig. 1. 2D Vectored Thrust Aircraft Free Body Diagram
Note: This diagram is not to scale.

C. Physics:

The aircraft can be represented as an airfoil that experiences aerodynamic forces (lift & drag) from the air pressure distribution and shear stresses. The lift force counteracts the weight of the aircraft, and the thrust reduces the drag. Based on Newton's 3^{rd} law, the applied downward thruster forces will have equal and opposite reactions, which are the aircraft lift forces. Also, the differential pressures across the aircraft area will create lift. The weight of the system is the aircraft mass. Drag is created by air and the vertical thruster reactions in the drag direction. The air stream leaving the thrusters is a laminar flow because the vertical maneuvers are at low speeds. The translational air drag, which opposes

the direction of motion, is equal to the velocity times the damping coefficient (c) ($F_{drag} = cx'$). Note that the 1^{st} derivative of the aircraft position is velocity. c depends on the frictional forces from the shear stresses along the aircraft surface and the air pressure distribution in the drag direction.

Newton's 2^{nd} law of motion is valid for this dynamic model because the aircraft's position and orientation change in time. This law states the summation of forces equals the mass times acceleration. Similarly, the summation of torques equals the moment of inertia times angular acceleration. Note that the 2^{nd} derivative of position is the aircraft acceleration. Based on the FBD in Fig. 1, the system forces are air drag, reaction forces by the thrusters, and weight. These forces are broken down into their respective x and y components (Equations 1 & 2). Note that these model equations apply to a hovering aircraft with no external disturbances. For Equation 3, the only torque on the aircraft is from the thruster reaction (F_1). Note that there is no air torque resistance in Equation 3.

D. Nonlinear Differential Equations [1]:

$$mx'' = F_1 cos\theta - F_2 sin\theta - cx' \tag{1}$$

$$my'' = F_1 sin\theta + F_2 cos\theta - mg - cy' \tag{2}$$

$$J\theta'' = rF_1 \tag{3}$$

Fig. 2 shows a nonlinear block diagram in Simulink.
Note: u_1 and u_2 represent F_1 and F_2 respectively in this block diagram.

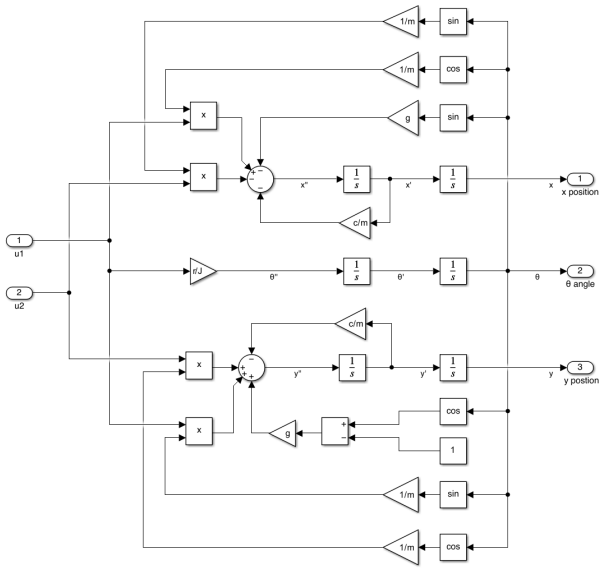

Fig. 2. Nonlinear Block Diagram

E. Nonlinear Differential Equation Observations:

This model has three coupled 2^{nd} order, ordinary differential equations. Note that these nonlinear equations have trigonometric functions. This system of equations is a continuous time model and a time-varying system because the response and the differential equation coefficients depend on time. The model is causal because the equations depend on the current states. As previously mentioned, this is a dynamic system as the aircraft's position and orientation change with respect to time. Table I lists the mathematical variables used in this analysis.

TABLE I
MATHEMATICAL VARIABLES

Variables	***Variable Name***	***Units***
x	aircraft horizontal position	m
x'	aircraft horizontal velocity	m/s
x''	aircraft horizontal acceleration	m/s^2
y	aircraft vertical position	m
y'	aircraft vertical velocity	m/s
y''	aircraft vertical acceleration	m/s^2
θ	aircraft angular position	rad
θ'	aircraft angular velocity	rad/s
θ''	aircraft angular acceleration	rad/s^2
J	moment of inertia	$kg * m^2$
r	distance from aircraft centroid to thrusters' intersection	m
c	damping coefficient	Ns/m
g	acceleration due to gravity	m/s^2
m	aircraft mass	kg
F_1	aircraft horizontal reaction	N
F_2	aircraft vertical reaction	N
y_e	y equilibrium point	m
x_e	x equilibrium point	m
z_e	state-space equilibrium points	–
F_e	input equilibrium points	N
A, B, C, D	state-space matrices	–
ζ	linearized state-space variable	–
v	linearized state-space input	–
P	linearized state-space output	–
z	nonlinear state-space variable	–
f	time derivative of z	–
h	nonlinear state-space output	–
F	nonlinear state-space input	–.
G_1	Local x transfer function	–
G_2	Local y transfer function	–

III. Analysis

This model is a system of nonlinear differential equations. Therefore, the system will be linearized around its equilibrium points with the Jacobian Linearization method [2]. These 2^{nd} differential equations are converted to a nonlinear state-space system, which is a system of 1^{st} order differential equations. z is the nonlinear state-space variable for the state equation: (z = ($z_1 = x$, $z_2 = y$, $z_3 = \theta$, $z_4 = x'$, $z_5 = y'$, $z_6 = \theta'$)), and F is the nonlinear input variable: (F = (F_1, F_2)).

Note: assume a small angle approximation around the equilibrium points: $sin(\theta) \approx \theta$ & $cos(\theta) \approx 1$. The range of θ is from 0 to 2π. Equations 4 and 5 show the nonlinear state-space and output equations respectively [1]. f is the time derivative of z, and h is the nonlinear state-space output.

$$f(z,F) = \frac{dz}{dt} = \begin{pmatrix} z_4 \\ z_5 \\ z_6 \\ -\frac{c}{m}z_4 + \frac{F_1}{m} - \frac{F_2 z_3}{m} \\ -g - \frac{c}{m}z_5 + \frac{F_1 z_3}{m} + \frac{F_2}{m} \\ \frac{r}{J}F_1 \end{pmatrix} \tag{4}$$

$$h = \begin{pmatrix} z_1 \\ z_2 \end{pmatrix} \tag{5}$$

A. Finding the Equilibrium Points:

The equilibrium points are determined by setting these nonlinear system of equations (Equations 4 & 5) to zero and solving for each z and F variable.

Stable Equilibrium Points:

z_e = ($z_1 = x_e$, $z_2 = y_e$, $z_3 = 0$, $z_4 = 0$, $z_5 = 0$, $z_6 = 0$)

F_e = ($F_1 = 0$, $F_2 = mg$)

Note: the system of equations above is independent of x and y.

At a given equilibrium point (x_e & y_e), there is no rotational or translational velocity, and the horizontal reaction force (F_1) and θ are zero. The vertical reaction force (F_2) supports its weight.

B. Jacobian Matrices:

Equations 6 and 7 compute the Jacobian Matrices for this nonlinear system [1].

$$A = \left.\frac{\partial f}{\partial z}\right|_{(z_e,F_e)} \quad B = \left.\frac{\partial f}{\partial F}\right|_{(z_e,F_e)} \tag{6}$$

$$C = \left.\frac{\partial h}{\partial z}\right|_{(z_e,F_e)} \quad D = \left.\frac{\partial h}{\partial F}\right|_{(z_e,F_e)} \tag{7}$$

The following 8-11 equations break down the Jacobian Matrices into the partial derivatives of f and h with respect to the nonlinear state-space variable (z) and nonlinear state-space input (F).

$$A = \begin{bmatrix} \frac{\partial f_1}{\partial z_1} & \frac{\partial f_1}{\partial z_2} & \frac{\partial f_1}{\partial z_3} & \frac{\partial f_1}{\partial z_4} & \frac{\partial f_1}{\partial z_5} & \frac{\partial f_1}{\partial z_6} \\ \frac{\partial f_2}{\partial z_1} & \frac{\partial f_2}{\partial z_2} & \frac{\partial f_2}{\partial z_3} & \frac{\partial f_2}{\partial z_4} & \frac{\partial f_2}{\partial z_5} & \frac{\partial f_2}{\partial z_6} \\ \frac{\partial f_3}{\partial z_1} & \frac{\partial f_3}{\partial z_2} & \frac{\partial f_3}{\partial z_3} & \frac{\partial f_3}{\partial z_4} & \frac{\partial f_3}{\partial z_5} & \frac{\partial f_3}{\partial z_6} \\ \frac{\partial f_4}{\partial z_1} & \frac{\partial f_4}{\partial z_2} & \frac{\partial f_4}{\partial z_3} & \frac{\partial f_4}{\partial z_4} & \frac{\partial f_4}{\partial z_5} & \frac{\partial f_4}{\partial z_6} \\ \frac{\partial f_5}{\partial z_1} & \frac{\partial f_5}{\partial z_2} & \frac{\partial f_5}{\partial z_3} & \frac{\partial f_5}{\partial z_4} & \frac{\partial f_5}{\partial z_5} & \frac{\partial f_5}{\partial z_6} \\ \frac{\partial f_6}{\partial z_1} & \frac{\partial f_6}{\partial z_2} & \frac{\partial f_6}{\partial z_3} & \frac{\partial f_6}{\partial z_4} & \frac{\partial f_6}{\partial z_5} & \frac{\partial f_6}{\partial z_6} \end{bmatrix}\Bigg|_{(z_e,F_e)} \tag{8}$$

$$B = \begin{bmatrix} \frac{\partial f_1}{\partial F_1} & \frac{\partial f_1}{\partial F_2} \\ \frac{\partial f_2}{\partial F_1} & \frac{\partial f_2}{\partial F_2} \\ \frac{\partial f_3}{\partial F_1} & \frac{\partial f_3}{\partial F_2} \\ \frac{\partial f_4}{\partial F_1} & \frac{\partial f_4}{\partial F_2} \\ \frac{\partial f_5}{\partial F_1} & \frac{\partial f_5}{\partial F_2} \\ \frac{\partial f_6}{\partial F_1} & \frac{\partial f_6}{\partial F_2} \end{bmatrix}\Bigg|_{(z_e,F_e)} \tag{9}$$

$$C = \begin{bmatrix} \frac{\partial h_1}{\partial z_1} & \frac{\partial h_1}{\partial z_2} & \frac{\partial h_1}{\partial z_3} & \frac{\partial h_1}{\partial z_4} & \frac{\partial h_1}{\partial z_5} & \frac{\partial h_1}{\partial z_6} \\ \frac{\partial h_2}{\partial z_1} & \frac{\partial h_2}{\partial z_2} & \frac{\partial h_2}{\partial z_3} & \frac{\partial h_2}{\partial z_4} & \frac{\partial h_2}{\partial z_5} & \frac{\partial h_2}{\partial z_6} \end{bmatrix}\Bigg|_{(z_e,F_e)} \tag{10}$$

$$D = \begin{bmatrix} \frac{\partial h_1}{\partial F_1} & \frac{\partial h_1}{\partial F_2} \\ \frac{\partial h_2}{\partial F_1} & \frac{\partial h_2}{\partial F_2} \end{bmatrix}\Bigg|_{(z_e,F_e)} \tag{11}$$

C. Linearized State-Space Equations & Block Diagram:

These Jacobian Matrices (Equations 14-17) create a linearized state-space system, which analyzes the local behavior around the equilibrium points [1]. New variables are created by subtracting the nonlinear state-space variable and input with its equilibrium points. Thus, $\zeta = z - z_e$ which is the linearized state-space variable, $v = F - F_e$, which is the linearized state-space input variable, and P is the linearized state-space output variable. Equations 12 and 13 show the linearized state-space and output equations respectively [1].

$$\zeta' = A\zeta + Bv \tag{12}$$

$$P = C\zeta + Dv \tag{13}$$

$$A = \begin{bmatrix} 0 & 0 & 0 & 1 & 0 & 0 \\ 0 & 0 & 0 & 0 & 1 & 0 \\ 0 & 0 & 0 & 0 & 0 & 1 \\ 0 & 0 & -g & -c/m & 0 & 0 \\ 0 & 0 & 0 & 0 & -c/m & 0 \\ 0 & 0 & 0 & 0 & 0 & 0 \end{bmatrix} \tag{14}$$

$$B = \begin{bmatrix} 0 & 0 \\ 0 & 0 \\ 0 & 0 \\ 1/m & 0 \\ 0 & 1/m \\ r/J & 0 \end{bmatrix} \tag{15}$$

$$C = \begin{bmatrix} 1 & 0 & 0 & 0 & 0 & 0 \\ 0 & 1 & 0 & 0 & 0 & 0 \end{bmatrix} \tag{16}$$

$$D = \begin{bmatrix} 0 & 0 \\ 0 & 0 \end{bmatrix} \tag{17}$$

For reference, the following 18-25 equations show each linearized state and output equation.

Linearized State Equations:

$$\zeta_1' = x' \tag{18}$$

$$\zeta_2' = y' \tag{19}$$

$$\zeta_3' = \theta' \tag{20}$$

$$\zeta_4' = -g\theta - c/mx' + v_1/m \tag{21}$$

$$\zeta_5' = -c/my' + v_2/m \tag{22}$$

$$\zeta_6' = (r/J)v_1 \tag{23}$$

Linearized Output Equations:

$$P_1 = \zeta_1 = x - x_e \tag{24}$$

$$P_2 = \zeta_2 = y - y_e \tag{25}$$

Fig. 3 displays a linearized block diagram in Simulink. Note: u_1 and u_2 represent F_1 and F_2 respectively in this block diagram.

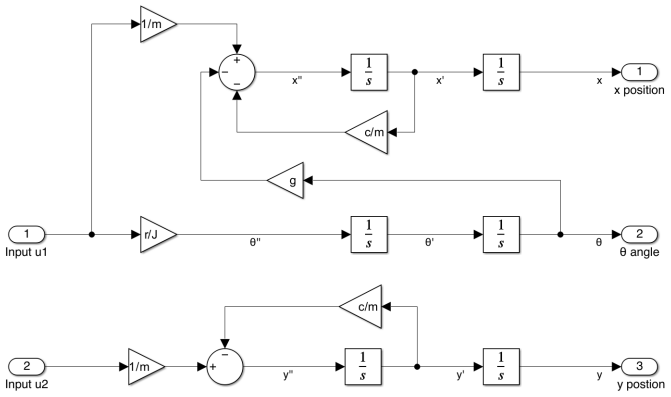

Fig. 3. Linearized Block Diagram

IV. Simulation

The simulation outputs are the local behaviors of the horizontal $(x - x_e)$ and vertical $(y - y_e)$ aircraft positional responses around their equilibrium points. As previously mentioned, this simulation will start at its equilibrium point $(x_e,\ y_e)$, and the aircraft is already supporting its weight at this location. The origin of this equilibrium point is $(x_e = 0,\ y_e = 0)$. The test inputs of the simulation are a sine wave at high & low frequencies, impulse, and step. Note that the simulation frequencies ($\omega_{low} = 0.01\ rad/s$, $\omega_{high} = 1000\ rad/s$) were chosen to capture the system dynamic at high and low frequencies. The following model parameters (Table II) are additionally used in this simulation:

TABLE II
Simulation Parameters [1]

m	4 kg
c	0.05 Ns/m
g	9.81 m/s^2
J	0.0475 kgm^2
r	0.25 m

A. Linearized Transfer Functions, Poles, & Zeros:

For this simulation, a MATLAB script converts these linearized Jacobian Matrices to a state-space system and transfer functions. The poles and zeroes are computed to determine the stability and system performance. For each transfer function, a Bode plot and the responses of the different inputs are plotted.

MATLAB converts these state-space equations to a transfer function for each output (Equation 26). Note that there are no initial conditions.

$$\frac{Y(s)}{U(s)} = C(sI - A)^{-1}B + D \tag{26}$$

The following shows the poles, zeros, and transfer functions (Equations 27 & 28) for the local behaviors of the vertical $(y - y_e)$ and horizontal $(x - x_e)$ positions around its equilibrium points.

Horizontal Positional $(x - x_e)$ Transfer Function:

$$G_1(s) = \frac{0.25s^4 + 0.003125s^3 - 51.63s^2 - 0.6454s}{s^6 + 0.025s^5 + 0.0001563s^4} \tag{27}$$

x Poles: 0, 0, 0, -0.0125, and -0.0125
x Zeros: 0, 14.3710, -14.3710, and -0.0125

Vertical Positional $(y - y_e)$ Transfer Function:

$$G_2(s) = \frac{0.25s^4 + 0.003125s^3}{s^6 + 0.025s^5 + 0.0001563s^4} \tag{28}$$

y Poles: 0, 0, 0, 0, -0.0125, and -0.0125
y Zeros: 0, 0, 0 , -0.0125

For both transfer functions, multiple poles at the origin make this system not asymptotically stable without accounting for pole-zero cancellation. For a step & impulse input, the local x transfer function has one pole-zero cancellation at the origin, but the multiplicity of the eigenvalues at the origin will cause this system to be unstable. The local y transfer function has 3 pole-zero cancellations at the origin, therefore the system responses will behave like a 2^{nd} order system. For this local y response, the impulse input will be a stable step response, and the step input will behave like an unstable ramp response.

V. Results

The following results are the Bode plots and the local behavior of the vertical $(y - y_e)$ and horizontal $(x - x_e)$ positional responses for these inputs (an impulse, a step, and a sine wave at different frequencies).

Note: A sinusoidal output will have the same frequency as the input but shifted in magnitude and phase. For a Bode plot, if the magnitude is greater than 0, the output will be amplified, and when the magnitude is less than 0, the signal will attenuate. The output amplitude is the same as the input amplitude if the magnitude is zero. A negative phase means the output leads the input, and the output lags the input for a positive phase. The output and input are in-phase when the phase is zero.

A. Local x Responses:

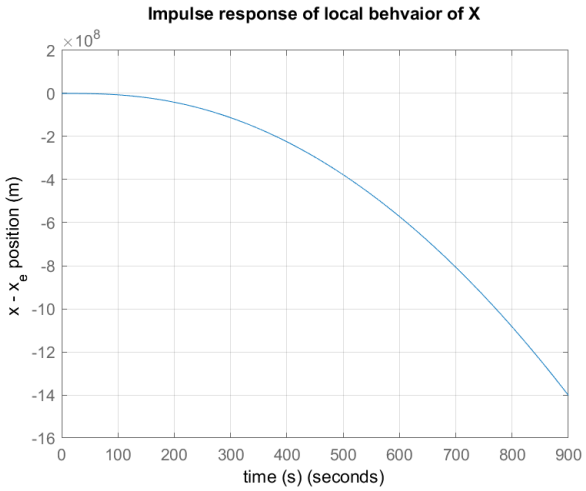

Fig. 4. Impulse x Positional Response

1) Local x Impulse Response: Fig. 4 shows the system initially starting at the origin and then going to negative infinity. Based on Equation 21, the magnitudes of air drag and weight were larger than the impulse input, therefore the trajectory traveled to the negative x direction. In the torque equation (Equation 23), the angular acceleration is directly proportional to the input. This equation does not have any torque resistance, so this system will continually rotate as θ increases. The small angle approximation assumption is no longer valid for large angle changes. This system is unstable but implementing a controller to bound θ.

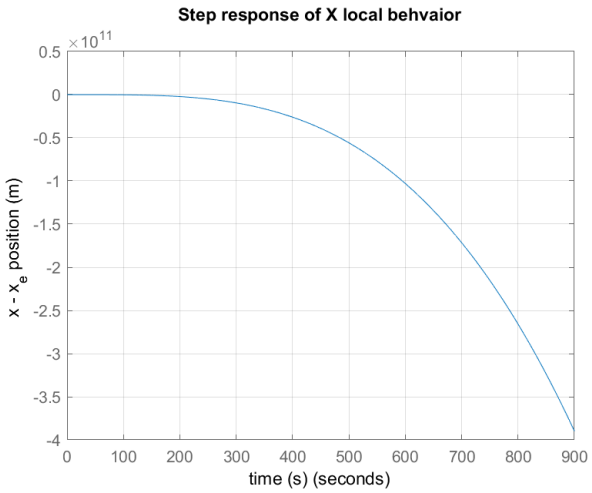

Fig. 5. Step x Positional Response

2) Local x Step Response: Fig. 5 has a similar trend as the impulse response. Initially, the step input had a longer constant response than the impulse response, but air drag and gravity changed the trajectory direction as θ increased. Note that the step input is constant, therefore a constant acceleration will create a parabolic response for local x. The moment of inertia, J, is indirectly proportional to the angular acceleration (Equation 23), so a small J will rapidly increase the angular acceleration. Note that this simulation captures the system response for the model and a real aircraft.

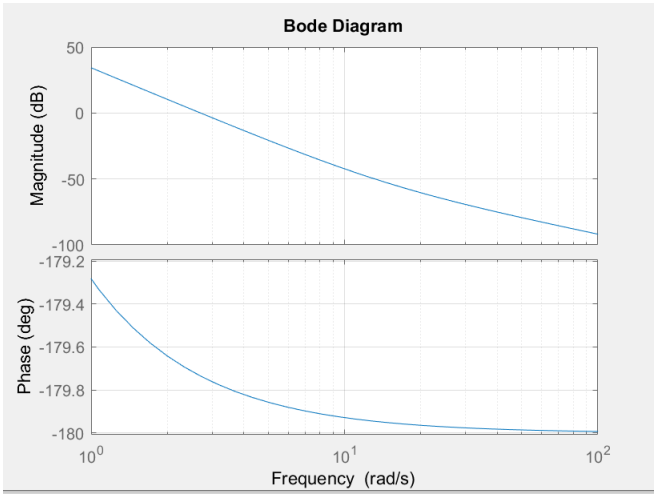

Fig. 6. Local x Bode Plot

3) Local x Bode Response: In Fig. 6, the magnitude is a constant slope, and the phase is an exponential decay for low frequencies. The output magnitude will be amplified, and lead the input signal. For high frequencies, the output signal will lead the input signal at a -180° phase, and its magnitude will attenuate with a smaller slope than the low frequencies. Note that the frequency range is from 1 to 1000 rad/s. This plot may not accurately represent the behavior at low frequency (0.01 rad/s).

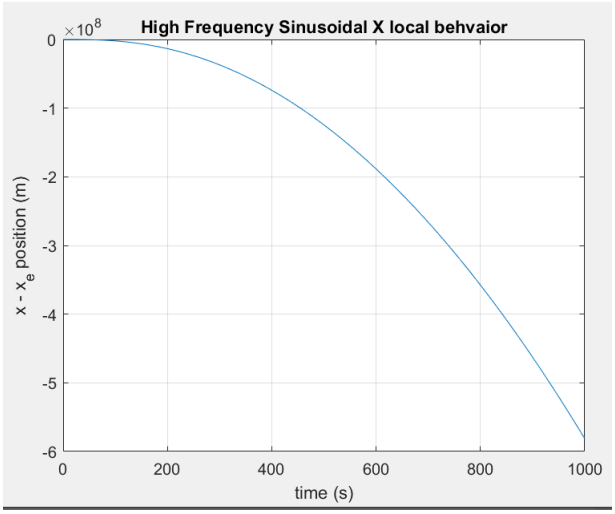

Fig. 7. High Frequency Sinusoidal x Positional Response

4) Local x High Freq Response: For high frequency (Fig. 7), the local behavior of x is similar to the step response. This response agrees with the Bode plot because the signal attenuates at a smaller slope than the low frequency response. As previously mentioned, this linearized system will go in the direction of negative infinity as it is unstable.

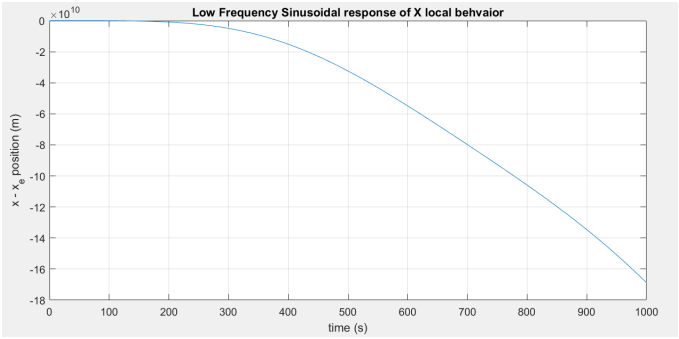

Fig. 8. Low Frequency Sinusoidal x Positional Response

5) Local x Low Freq Response: Fig. 8 displays an identical trajectory as the impulse response. This response agrees with the Bode plot as the change in position is larger than the high frequency response. As previously mentioned, there is no torque resistance, so the system will tend in the direction of negative infinity.

B. Local y Responses:

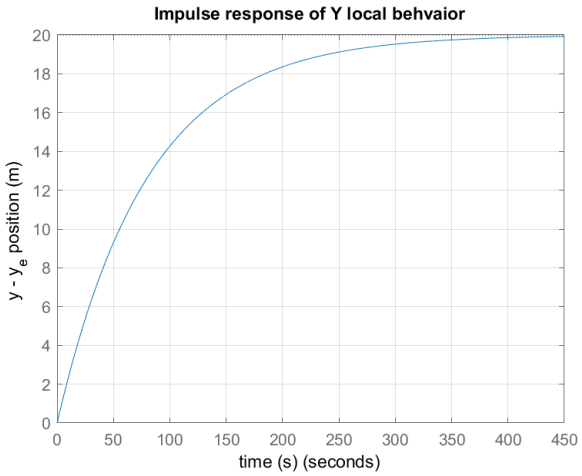

Fig. 9. Impulse y Positional Response

1) Local y Impulse Response: Fig. 9 shows the impulse initially accelerating the aircraft before reaching a steady state position. As previously mentioned, an impulse input is expected to be a stable step response. In comparison to the local x response, the local y response is independent of θ (Equation 22). Therefore, air drag is the only component slowing down the input.

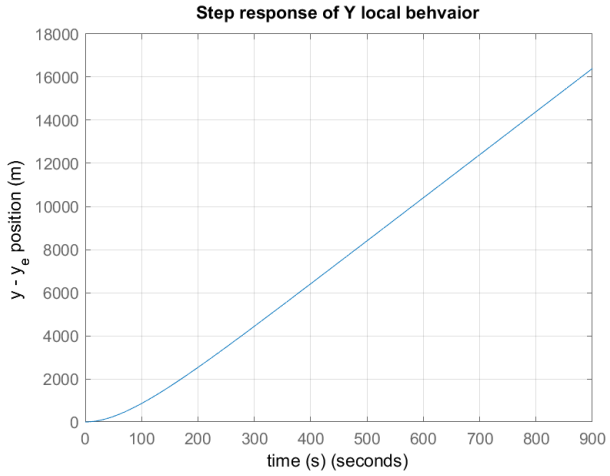

Fig. 10. Step y Positional Response

2) Local y Step Response: In Fig. 10, the local y behavior is linear because the system reached a constant terminal velocity. Thus, the step input is constant and larger than the air drag, so this system will tend to the direction of positive infinity. As previously mentioned, the local y transfer function shows the step input will behave like an unstable ramp response.

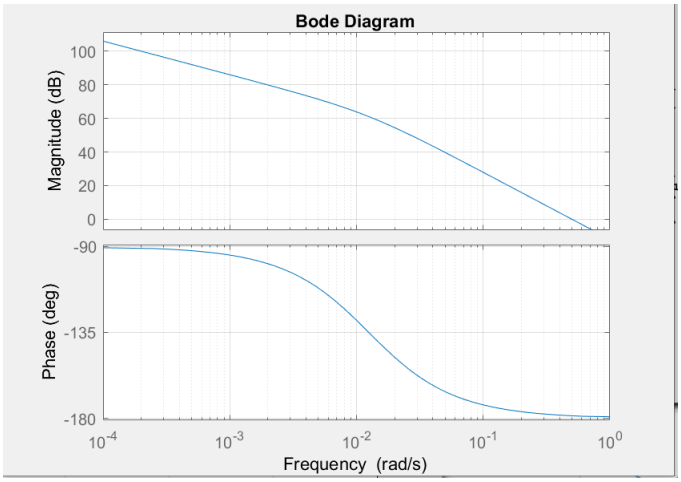

Fig. 11. Local y Bode Plot

3) Local y Bode Response: Fig. 11 illustrates the output magnitude is amplified and has a constant slope at low frequencies. At high frequencies, the magnitude slope becomes more steep. This amplified signal gradually attenuates at higher frequencies. The output response leads the input because the phase plot is negative. The signal changes from a -90° phase at low frequencies to a -180° phase at high frequencies. Note that the frequency range is from 0.0001 to 1 rad/s. This plot may not accurately represent the behavior at high frequency (1000 rad/s).

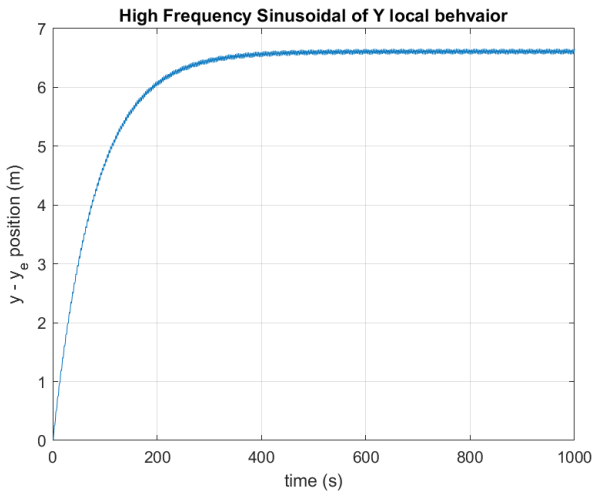

Fig. 12. High Frequency Sinusoidal y Positional Responsee

4) Local y High Freq Response: The graph (Fig. 12) is similar to the impulse response. At high frequencies, the local y response is initially amplified and slowly attenuates periodically to a steady-state mean. The system reaches a steady-state mean because air drag is slowing down the aircraft.

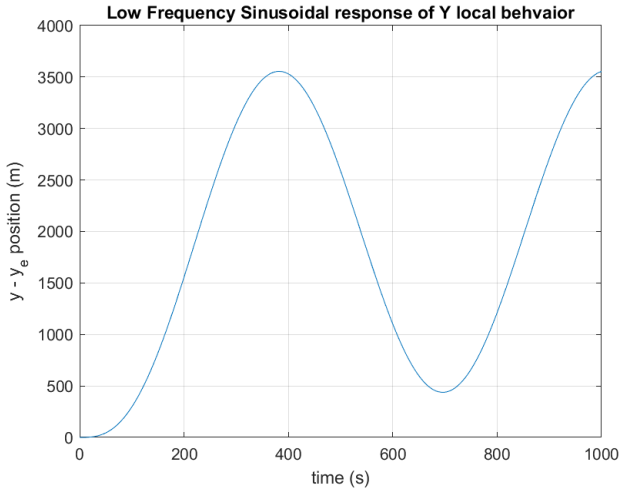

Fig. 13. Low Frequency Sinusoidal y Positional Response

5) Local y Low Freq Response: For low frequencies, the output signal will be amplified and gradually decrease its amplification over time (Fig. 13). This response converges faster to a steady-state mean than the high frequencies because the slope changes at this simulated frequency in the Bode plot.

VI. Limitations and Future Improvements

The limitations of the model are neglecting air torque resistance and violating the small angle approximation. Note that linearizing the system around its equilibrium points may not capture the majority of the nonlinear system dynamics. For future applications, a LQR controller can be implemented to control external disturbances and stability. The model can include vertical takeoff and landing maneuvers.

VII. Group Contribution Breakdown

Reese: FBD, Nonlinear and Linear Simulink Models, Block Diagram photos, and interpretation/analysis of the Linear/Nonlinear results to the physical system.

Sayed: Nonlinear Simulink model, Linearizing Nonlinear System, Analysis, and Mathematical Reviewer.

Tyler: Linearizing Nonlinear System, References, Analysis, MATLAB Simulation, and create an Overleaf template with Model equations, Analysis, Simulation, and MATLAB Results.

VIII. References

[1] K. J. Åström, R. M. Murray, *Feedback Systems: An Introduction for Scientists and Engineers.* Princeton University Press, 2008. [Online]. Available: http://www.cds.caltech.edu/∼murray/books/AM08/pdf/fbs-public_24Jul2020.pdf. Accessed: Feb. 10, 2024.

[2] A. D. Lewis and D. R. Tyner, "Geometric Jacobian linearization and LQR theory," Journal of Geometric Mechanics, vol. 2, no. 4, pp. 397–440, 2010, Accessed on: Feb. 10, 2024. [Online]. Available: https://doi.org/10.3934/jgm.2010.2.397.

[3] K.K. S. Kumar, H. Arya, A. Joshi, "Automatic Control of Harrier Maneuver of an Agile Fixed-Wing UAV," Indian Control Conference (ICC), IEEE, 2019. Accessed on: Feb. 10, 2024. [Online]. Available: https://ieeexplore.ieee.org/document/8715566.